

## FORCED OSCILLATIONS OF A GAS BUBBLE IN A SPHERICAL VOLUME OF A COMPRESSIBLE LIQUID

R. I. Nigmatulin, I. Sh. Akhatov, and N. K. Vakhitova

UDC 533.2

*A spherically symmetric problem of oscillations of a single gas bubble at the center of a spherical flask filled with a compressible liquid under the action of pressure oscillations on the flask wall is considered. A system of differential-difference equations is obtained that extends the Rayleigh–Plesset equation to the case of a compressible liquid and takes into account the pressure-wave reflection from the bubble and the flask wall. A linear analysis of solutions of this system of equations is performed for the case of harmonic oscillations of the bubble. Nonlinear resonance oscillations and nearly resonance nonharmonic oscillations of the bubble caused by harmonic pressure oscillations on the flask wall are analyzed.*

**Introduction.** Let us consider the spherically symmetric motion of a compressible liquid in a spherical flask of radius  $R$  about a spherical gas bubble located at the center of the flask.

If the pressure perturbations are small so that liquid-pressure variations can be ignored, and the wavelength of the liquid ultimate is much greater than the bubble radius, an incompressible liquid approximation is usually employed for the mathematical modeling of the bubble oscillations. In this case, the equation of liquid motion around the bubble is reduced to the known Rayleigh–Plesset equation [1–3]

$$a \frac{dw_a}{dt} + \frac{3}{2} w_a^2 = \frac{p_a - p_\infty}{\rho}, \quad w_a = \frac{da}{dt}, \quad p_a = p_g(a) - \frac{2\sigma}{a} - \frac{4\mu w_a}{a}, \quad (1)$$

where  $a$  is the bubble radius,  $\rho$ ,  $\mu$ , and  $\sigma$  are the density, viscosity, and surface-tension coefficient of the liquid, respectively,  $w_a$  and  $p_a$  are the radial velocity and pressure of the liquid at the bubble surface,  $p_g$  is the gas pressure in the bubble, and  $p_\infty$  is the liquid pressure away from the bubble.

Previously, the effect of the liquid compressibility on bubble oscillations was taken into account by introducing the so-called losses in acoustic radiation [2, 3], which led to the Herring–Gilmore equation

$$a \frac{dw_a}{dt} + \frac{3}{2} w_a^2 = \frac{p_a - p_\infty}{\rho} + \frac{a}{\rho c} \frac{d(p_a - p_\infty)}{dt} \quad (2)$$

( $c$  is the speed of sound in the liquid).

The dynamics of cavitation bubbles in a supersonic field for both compressible and incompressible liquids was analyzed in detail in [4, 5]. An approximate theory of radial oscillations of a spherical bubble in an infinite, weakly compressible liquid under the action of an acoustic field was developed in [6, 7]. A system of equations including Eq. (2) and other equations from [2, 3] as particular cases was obtained. It is shown that all these equations are equivalent since they have the same order of accuracy for the liquid Mach number. In the derivation of these equations it was assumed that bubble oscillations do not affect the acoustic pressure at infinity. Actually, since the liquid is infinite, the problem of bubble oscillations can be considered independently of the acoustic problem in the liquid.

In the work presented here, the coupled problem of oscillations of a limited liquid volume and a gas bubble is studied for the case where the flask wall is a source of liquid oscillations. It is shown that the bubble oscillations are described by a Herring–Gillmore-type equation, in which the external pressure (outside the bubble) is related to the bubble-radius variation and the pressure on the flask wall by a differential-difference equation. This external pressure differs from both the pressure at local infinity [ $p_\infty$  in Eq. (2)] and the pressure on the flask wall  $p_R$ .

**System of Equations for the Bubble Radius.** In the case of low Mach numbers ( $M_a = w_a/c \ll 1$ ), the space between the bubble surface and the flask wall can be divided into three zones:

1. An outer zone, where the weak compressibility of the liquid is essential but the nonlinear forces of inertia due to convective accelerations are negligibly small. In this zone, the motion of the liquid has a wave form and is characterized by a finite constant velocity of perturbation propagation.

2. An inner zone (near the bubble surface), where the liquid compressibility is negligibly small. In this zone, the nonlinear forces of inertia due to convective accelerations are significant and the liquid moves as a result of bubble compression and expansion.

3. An intermediate zone, where the liquid compressibility and the nonlinear forces of inertia are rather considerable.

To obtain an equation for the bubble-radius oscillations, it is necessary to join, in the intermediate zone, the asymptotic solutions for the outer and inner zones using the conditions of continuity for the flow and pressure. The required equation of bubble oscillations in a compressible liquid in a long-wave approximation has the form [8, 9]

$$a\ddot{a} + \frac{3}{2}\dot{a}^2 = \frac{p_a - p_0}{\rho} + \frac{1}{c}[2\ddot{\psi}_2(t) + \ddot{Q}(t)], \quad Q(t) = a^2\dot{a}, \quad (3)$$

where  $\psi_2$  is the part of the liquid-velocity potential that describes the wave propagating from the flask wall to the bubble, multiplied by the radial coordinate  $r$ , and  $p_0$  is the initial pressure in the flask. The pressure on the flask wall is related to  $\psi_2$  by the equation

$$p_R(t) = p_0 - \frac{\rho}{R} \left[ \dot{\psi}_2 \left( t + \frac{R}{c} \right) - \dot{\psi}_2 \left( t - \frac{R}{c} \right) - \dot{Q} \left( t - \frac{R}{c} \right) \right], \quad (4)$$

where  $R$  is the flask radius.

Equation (3) leads to the following expression for the pressure  $p_\infty$ , which is the pressure away from the bubble (at local infinity) in Eq. (1):

$$p_\infty = p_0 - \frac{\rho}{c} [2\ddot{\psi}_2(t) + \ddot{Q}(t)].$$

It is important that the solution depends on the third derivative of the bubble radius, as noted in [6]. However, in a long-wave approximation, for low Mach numbers one can use an asymptotic form without the third derivative for the term  $\ddot{Q}/c$ , which defines the bubble effect on the reflected wave. In this case, the evolution of the radius is described by the equation

$$\left(1 - \frac{\dot{a}}{c}\right)a\ddot{a} + \frac{3}{2}\left(1 - \frac{\dot{a}}{3c}\right)\dot{a}^2 = \left(1 - \frac{\dot{a}}{c}\right)\frac{p_a - p_I}{\rho} + \frac{a}{c}\frac{d}{dt}\left[\frac{p_a - p_I}{\rho}\right], \quad (5)$$

where  $p_I = p_0 - (2\rho/c)\ddot{\psi}_2$ . The system of ordinary differential-difference equations (4) and (5), comprising both the delayed and advanced potentials, is closed at specified density  $\rho$ , speed of sound  $c$ , surface tension  $\sigma$  and viscosity  $\mu$  of the liquid, the equation of state for the bubble gas  $p_g(a)$ , and the liquid pressure on the flask wall  $p_R(t)$ .

We note that gas supercompression and luminescence (sonoluminescence) can occur during bubble collapse, when the liquid compressibility approximation in the boundary layer near the bubble is invalid. Nevertheless, bubble collapse takes a very small fraction of the bubble oscillation period. In this time interval, it is necessary to take into account the liquid compressibility near the bubble wall and formation and propagation of shock waves in the liquid and gas [10].

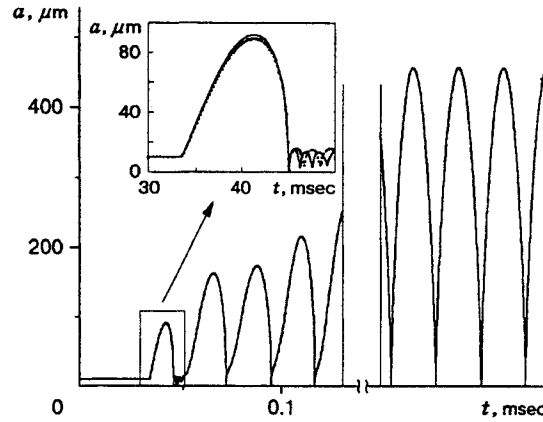


Fig. 1

**Direct Problem.** Let us consider the problem of the evolution of the bubble radius  $a(t)$  where the liquid-pressure variation on the flask wall  $p_R(t)$  is specified.

In the general case, a solution of the direct problem of bubble radius evolution can be obtained by numerical integration of the partial differential equations describing the motion and compression of the liquid and the gas, as was done in [10]. In [10], the problem was solved under the condition that the pressure on the flask wall varied according to the harmonic law

$$p_R(t) = \begin{cases} p_0, & t \leq 0, \\ p_0 - \Delta p_R \sin(\omega t), & t > 0. \end{cases} \quad (6)$$

Such a calculation requires high computer power. Because of lengthy computations, the evolution of the radius was found only for the first period of oscillations of the external pressure field but not for the periodic regime, which occurs after many periods of oscillations.

Figure 1 shows calculation results for the evolution of the radius of a gas bubble ( $a_0 = 10 \mu\text{m}$ ) in a flask ( $R = 5 \text{ cm}$ ) filled with water (initial conditions  $p_0 = 1 \text{ bar}$  and  $T_0 = 300 \text{ K}$ ) with the pressure on flask wall varying according to the harmonic law (6) with an amplitude of  $\Delta p_R = 0.25 \text{ bar}$  and frequency  $f = 45 \text{ kHz}$  ( $\omega = 2\pi f$ ). The first oscillation is in agreement with the calculation result of [10] (the dashed curve). However, calculation of the further evolution of the bubble radius shows that the second oscillation differs from the first, the third differs from the second, and a periodic regime occurs only after many oscillations ( $t \gg \omega^{-1}$ ). The long period of establishment is due to the high inertia of the liquid in the flask. Exactly the mass of the liquid ( $\sim \rho R^3$ ) delays realization of the periodic regime of pressure variation near the bubble (at local infinity)  $p_\infty$ . The delay of the periodic regime for bubble oscillations after establishment of the periodic regime for  $p_\infty$  is much shorter since it is determined by the attached mass of the liquid around the bubble ( $\sim \rho a^3 \ll \rho R^3$ ).

We note that precisely a periodic regime is observed in experiments on sonoluminescence [11] and, therefore, it is important and interesting to consider solutions that describe periodic oscillation regimes.

**Forced Linear Oscillations.** The problem has two characteristic frequencies: the flask resonance frequency  $\omega_R = \pi c/R$ , determined by the time of propagation of acoustic waves  $t_R = 2R/c$  at distance  $2R$  from the flask wall to its center and back, and the eigenfrequency of free oscillations of the bubble (Minaert's frequency)  $\omega_a = \sqrt{3\gamma p_0/a_0^2 \rho}$ .

Let us consider forced harmonic oscillations of the form  $A \exp(i\omega t)$  with angular frequency  $\omega$ . Then, the response function, calculated as the ratio of the relative amplitude of bubble-radius oscillations  $A_a = \Delta a/a_0$  to the relative amplitude of oscillations of the forcing pressure  $A_{p_R} = \Delta p_R/p_0$ , can be represented as a function of the nondimensional frequency  $\bar{\omega} = \omega(R/\pi c)$ . Figure 2 shows the amplitude-frequency response of harmonic oscillations of a bubble in a flask of radius 5 cm filled with water (in Fig. 2a, the solid curve is calculated for  $a_0 = 10 \mu\text{m}$  and  $\omega_a = 2.16 \cdot 10^6 \text{ sec}^{-1}$  and the dashed curve is calculated for  $a_0 = 500 \mu\text{m}$  and

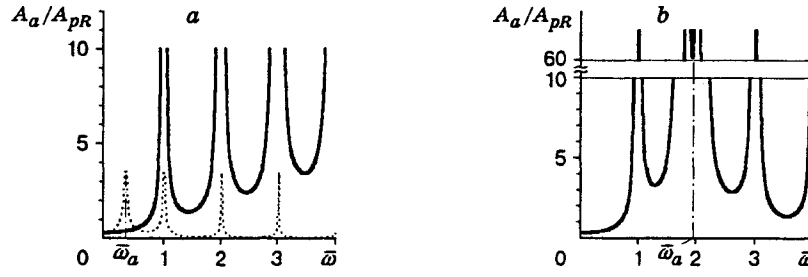


Fig. 2

$\omega_a = 41.03 \cdot 10^3 \text{ sec}^{-1}$ ; the curve in Fig. 2b is calculated for  $a_0 = 100 \text{ } \mu\text{m}$  and  $\omega_a = 2.06 \cdot 10^5 \text{ sec}^{-1}$ ).

As should be expected, resonance for the absolute value of the response function  $|A_a/A_{pR}|$  is observed at  $\bar{\omega} \approx 1, 2, 3, \dots$ . This is flask resonance:  $\omega_k = 2\pi f_k = k\pi c/R = k\omega_R$  ( $k = 1, 2, 3, \dots$ ) and, when the bubble is rather small, it cannot significantly change the resonance frequencies. Thus, for a flask of radius  $R = 5 \text{ cm}$  filled with water, the first resonance frequency is  $f_1 \approx 15 \text{ kHz}$  ( $\omega_1 = 94.2 \cdot 10^3 \text{ sec}^{-1}$ ).

The influence of the bubble on the resonance frequencies is marked only when the excitation frequency of the flask wall is comparable to the Minaert frequency of bubble oscillations  $\omega_a$  (the curves in Fig. 2 calculated for  $a_0 = 100$  and  $500 \text{ } \mu\text{m}$ ).

It is interesting that the smaller the bubble, the greater the response  $|A_a/A_{pR}|$  (compare the curves in Fig. 2 for  $a_0 = 10$  and  $500 \text{ } \mu\text{m}$ ). This is proved by sonoluminescence of very small bubbles ( $a_0 = 4\text{--}10 \text{ } \mu\text{m}$ ).

For forced oscillations with frequencies close to the resonance frequencies, a nonlinear analysis is required, where there is large-amplitude nonharmonic response of the bubble radius to external action  $\Delta a \sim a$ , which is possible even for small sinusoidal oscillations of the flask-wall pressure  $\Delta p_R \ll p_0$ .

**Nonlinear Analysis of Resonance Frequencies.** Nonlinear periodic solutions for the flask resonance  $\omega = \omega_k = k\pi c/R$  ( $k = 1, 2, 3, \dots$ ) are obtained. For the periodic regime caused by sinusoidal pressure oscillations on the flask wall  $p_R(t) = p_0 - \Delta p_R \sin(\omega_k t)$ , the nonlinear periodic solution has the form

$$a^3 = a_*^3 \left\{ 1 + c_* + \sin \left[ \omega_k \left( t + \frac{R}{c} \right) \right] \right\}, \quad a_*^3 = \frac{3R^3 A_{pR} p_0}{\pi^2 k^2 \rho c^2}, \quad 0 < c_* \ll 1, \quad a_{\max}^3 \approx 2a_*^3. \quad (7)$$

The solution should be treated as an ideal periodic regime since it is obtained for the limiting case of an ideal, weakly compressible liquid and an incompressible boundary layer around the bubble, which assumes the absence of any dissipation mechanism.

The exact value of the integration constant  $c_*$  is determined numerically from the condition that the flask-wall velocity and its motion are also periodic. The solution has the important parameter  $a_*$ , which determines the maximum bubble radius  $a_{\max}$ , which, in practice, does not depend on the initial radius  $a_0$  for the ideal resonance regime. In order that bubble collapse and sonoluminescence proceed in the resonance regime, the condition  $a_{\min} \ll a_0 \ll a_{\max} \sim a_*$  must be satisfied. However, one should take into account that the minimum value of the bubble radius  $a_{\min}$  cannot be considered physically realizable since for strong compression, the Mach number cannot be considered low.

The ideal periodic resonance regime shown in the right part of Fig. 1 corresponds to the third flask resonance  $f = f_3 = 45 \text{ kHz}$ . In this case, the maximum radius is  $a_{\max} = 454 \text{ } \mu\text{m}$ , which is in agreement with Eq. (7).

For small deviations from the resonance frequencies  $\omega = \omega_k + \Delta\omega$ , and  $\Delta\omega \ll \omega_k$ , where  $\omega_k = \pi kc/R$  ( $k = 1, 2, 3, \dots$ ), the bubble-radius oscillations under periodic perturbations are described by the equation

$$\begin{aligned} & \left( 1 - \frac{a\omega_k}{R\Delta\omega} \right) a\ddot{a} + \left( \frac{3}{2} - 2\frac{a\omega_k}{R\Delta\omega} \right) \dot{a}^2 \\ & = \frac{p_a - p_0}{\rho} - \frac{1}{\rho} \frac{\omega_k}{\Delta\omega} \Delta p_R \left( t + \frac{R}{c} \right) + \frac{a}{\rho c} \frac{d}{dt} \left[ p_a - p_0 - \frac{\omega_k}{\Delta\omega} \Delta p_R \left( t + \frac{R}{c} \right) \right]. \end{aligned} \quad (8)$$

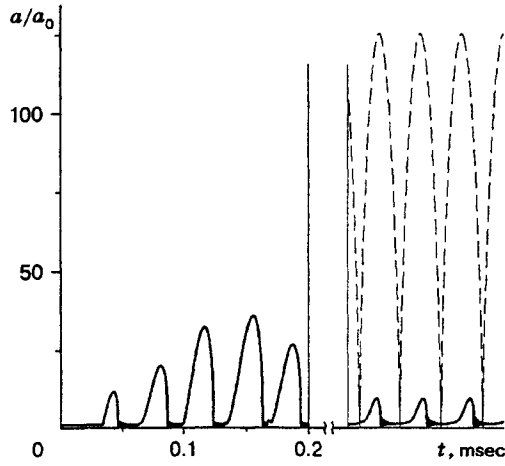


Fig. 3

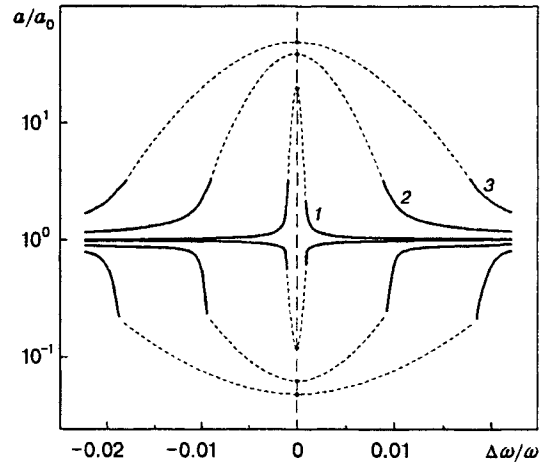


Fig. 4

This equation includes an important nondimensional parameter that describes bubble oscillations in the near-resonance regime:

$$A_* = \frac{a_0 \omega_k}{R \Delta \omega},$$

which is the product of the small parameter  $a_0/R$  and the large  $\omega_k/\Delta\omega$  parameters. Equation (8) is obtained under the assumption that  $A_* \ll 1$ . In this case, in contrast to the resonance case ( $\Delta\omega = 0$ ), the bubble pressure determines its oscillations. For  $\Delta\omega \rightarrow 0$  ( $A_* \rightarrow \infty$ ), Eq. (8) is reduced to Eq. (7) for the resonance case.

Figure 3 shows calculation results for the characteristic near-resonance regime of bubble oscillations ( $a_0 = 4 \mu\text{m}$ ) in a flask ( $R = 5 \text{ cm}$ ) filled with water ( $p_0 = 1 \text{ bar}$  and  $T_0 = 300 \text{ K}$ ) with the pressure on the flask wall varying by the harmonic law (6) with an amplitude  $\Delta p_R = 0.15 \text{ bar}$  and frequency  $f = 26.5 \text{ kHz}$ . The solid curve to the right shows the ideal periodic regime close to the resonance case ( $f \approx f_2$ ,  $\Delta f = -3.5 \text{ kHz}$ , and  $\Delta\omega = -22 \cdot 10^3 \text{ sec}^{-1}$ ). The larger-amplitude oscillations correspond to the ideal resonance regime (the dashed curve).

Curves 1–3 in Fig. 4 represent the dependences of  $a_{\min}$  and  $a_{\max}$  on the frequency shift from the frequency of the third flask resonance for  $a_0 = 4 \mu\text{m}$  and  $\Delta p_R = 0.001, 0.01$ , and  $0.02 \text{ bar}$ , respectively. The resonance case ( $\Delta\omega = 0$ ) is shown by points. Near the resonance frequency, the results are shown by dashed curves since, in this region, Eq. (8) ceases to be valid.

**Heat-Transfer Effects.** The heat-transfer processes inside the bubble and the heat exchange between the bubble and the liquid can play an important role for oscillations of a gas bubble. For a detailed analysis of these processes, we use the model proposed in [12] (see also [3]). It is based on the following approximations:

- 1) The gas pressure in the bubble  $p_g$  is spatially uniform and depends only on time (homobaric conditions);
- 2) The liquid temperature differs little from its value in the unperturbed state  $T_0$ . Then, to find the gas pressure in the bubble, we use the equation

$$\frac{dp_g}{dt} = -\frac{3\gamma p_g \dot{a}}{a} + \frac{3(\gamma-1)}{a} \lambda_g \left. \frac{\partial T_g}{\partial r} \right|_{r=a}, \quad (9)$$

where the heat flux on the bubble surface is determined from the solution of the interior thermal problem:

$$c_p \rho_g \left( \frac{\partial T_g}{\partial t} + w_g \frac{\partial T_g}{\partial r} \right) = \frac{1}{r^2} \frac{\partial}{\partial r} \left( \lambda_g r^2 \frac{\partial T_g}{\partial r} \right) + \frac{dp_g}{dt}, \quad w_g = \frac{\gamma-1}{\gamma p_g} \lambda_g \frac{\partial T_g}{\partial r} - \frac{r}{3\gamma p_g} \frac{dp_g}{dt},$$

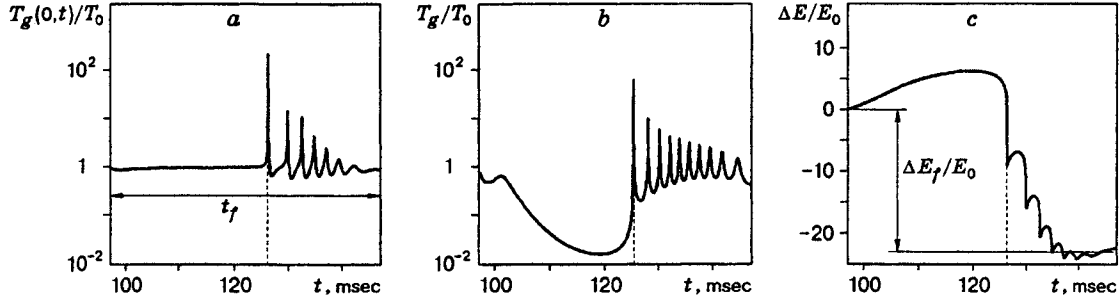


Fig. 5

$$p_g = c_{pg} \frac{\gamma - 1}{\gamma} \rho_g T_g, \quad T_g|_{r=a} = T_0, \quad \frac{\partial T_g}{\partial r}|_{r=0} = 0. \quad (10)$$

Here  $c_{pg}$ ,  $\lambda_g$ ,  $\gamma$ , and  $\rho_g$  are the specific heat (at constant pressure), thermal conductivity, Poisson's ratio, and gas density, respectively.

System (9), (10) was solved numerically simultaneously with Eqs. (5) for the radius, where  $p_a = p_g - 2\sigma/a$ . The external pressure was taken in the form  $p_I = p_0 - \Delta p_I \sin(\omega t)$ , lest the problem is solved in the full formulation and the relation between  $p_R$  and  $p_I$  is used.

The ordinary differential equations (5) and (9) were solved by the Runge-Kutta method of fifth-order accuracy, and the temperature distribution inside the bubble was obtained using an implicit scheme of the second order for time and space.

Figures 5 shows results of calculations for an argon bubble of radius  $10 \mu\text{m}$  oscillating with a frequency of 21 kHz and an amplitude of 1.5 bar under the action of pressure  $p_I$  for one oscillation period of this pressure ( $t_f = 2\pi/\omega$ ). One can see in Fig. 5a that during the major portion of the period, which corresponds to bubble expansion, the bubble remains isothermal [ $T_g(0,t) \approx T_0$ ]. In adiabatic expansion of the gas bubble, other conditions being the same (Fig. 5b), the bubble temperature would reach extremely small values ( $\sim 5$  K). In compression, the maximum temperature at the center of the bubble is much higher ( $\sim 68000$  K) than that for the adiabatic case ( $\sim 18000$  K). As an illustration of this phenomenon, Fig. 5c shows the total heat flux

from the liquid to the bubble  $\Delta E = \int_0^{t_f} 4\pi a^2 \lambda_g (\partial T / \partial r)_a dt$ , referred to the internal energy of the unperturbed bubble  $E_0 = (4/3)\pi a_0^3 \rho_g c_{gv} T_0$ . It can be seen that during expansion, the bubble draws a considerable portion of energy from the surrounding liquid (thermal pump). During compression, the bubble releases greater energy than that it previously drew from the liquid. The difference between the delivered and released energies is the energy loss by the system, defined as  $\Delta E_f/E_0$ .

This effect was first mentioned in [13] for larger bubbles and lower pressure amplitudes (0.93 bar), for which bubble compressions and expansions were not as strong as those in the given case, and the difference between the maximum temperatures calculated with allowance for the solution of the thermal problem and in an adiabatic approximation was much lower (3000 and 1328 K).

It is expected that the thermal pump effect would play an important role in oscillations of small ( $\sim 4 \mu\text{m}$ ) sonoluminescent bubbles.

**Conclusions.** (1) The bubble-oscillation process can be divided into two stages. The first stage corresponds to low Mach numbers, where the bubble's surface velocity is much lower than the speed of sound in the liquid; the second stage corresponds to the moments of rapid strong compression and rapid expansion of the bubble, where the bubble's surface velocity is comparable to or even exceeds the local speed of sound in the liquid.

The first stage takes almost the entire oscillation period ( $\sim 10^{-5}$  sec), and the second stage is very short ( $\sim 10^{-8}$  sec). Nevertheless, over this short period, bubble supercompression occurs and the temperature

inside the bubble increases to such an extent that luminescence of the gas is possible.

(2) For low Mach number regimes, two asymptotic relations are valid. The first asymptotic relation follows from the solution of the linear wave equation and describes the motion of the liquid away from the bubble; the second asymptotic relation describes the motion of the liquid in the boundary layer near the bubble and corresponds to the solution of the Laplace equation for an incompressible liquid.

(3) The forced oscillations of a bubble in a compressible liquid at low Mach numbers can be described by the Rayleigh–Plesset or Herring–Gilmore equations. However, in these equations, the external pressure, namely, the pressure at local infinity around the bubble  $p_\infty$  in the first equation and the external pressure  $p_I$  in the second equation, differ from each other and from the pressure on the flask wall. The pressures  $p_\infty$  and  $p_I$  can be calculated for a known law of pressure variation on the flask wall from an ordinary differential-difference equation, as shown in this paper.

4. The amplitudes of the pressure at local infinity  $\Delta p_\infty$  and the external pressure  $\Delta p_I$  can be much higher than the pressure amplitude on the flask wall  $\Delta p_R$ . This is a result of strengthening of spherical acoustic waves moving from the flask wall to the bubble. The greatest strengthening, completely or partially compensated by bubble expansion and compression, is observed at the flask resonance frequencies,

## REFERENCES

1. Lord Rayleigh, "On the pressure developed in a liquid during the collapse of a spherical cavity," *Philos. Mag.*, **34**, No. 200, 94–98 (1917).
2. R. Knapp, J. Daily, and F. Hammit, *Cavitation* [Russian translation], Mir, Moscow (1974).
3. R. I. Nigmatulin, *Dynamics of Multiphase Media*, Part 1, Hemisphere Publ., New York (1991).
4. V. A. Akulichev, "Pulsations of cavitation cavities," in: *Powerful Ultrasonic Fields* [in Russian], Part 4, Nauka, Moscow (1968), pp. 131–166.
5. M. I. Vorotnikova and R. I. Soloukhin, "Calculation of pulsations for gas bubbles in an incompressible liquid under the action of periodically varying pressure," *Acoust. J.*, **10**, No 1, 34–39 (1964).
6. A. Prosperetti and A. Lezzi, "Bubble dynamics in a compressible liquid, Part 1: First order theory," *J. Fluid Mech.*, **168**, 457–478 (1986).
7. A. Prosperetti and A. Lezzi, "Bubble dynamics in a compressible liquid. Part 2: Second order theory," *J. Fluid Mech.*, **185**, 289–304 (1987).
8. R. I. Nigmatulin, I. Sh. Akhatov and N. K. Vakhitova, "On the liquid compressibility in the dynamics of a gas bubble," *Dokl. Ross. Akad. Nauk*, **348**, No. 6, 768–771 (1996).
9. I. Sh. Akhatov, N. K. Vakhitova, G. Ya. Galeeva, et al., "On weak oscillations of a gas bubble in a spherical volume of a compressible liquid," *Prikl. Mat. Mekh.*, **61**, No. 6, 952–962 (1997).
10. W. C. Moss, D. B. Clarke, J. W. White, and D. A. Young, "Hydrodynamic simulation of bubble collapse and picosecond sonoluminescence," *Phys. Fluids*, **6**, No. 9, 2979–2985 (1994).
11. D. F. Gaitan, L. A. Crum, C. C. Chursh, and R. A. Roy, "Sonoluminescence and bubble dynamics for a single, stable, cavitation bubble," *J. Acoust. Soc. Amer.*, **91**, No. 6, 3166–3181 (1991).
12. R. I. Nigmatulin and N. S. Khabeev, "Heat exchange of a gas bubble and a liquid," *Izv. Akad. Nauk SSSR, Mekh. Zhidk. Gaza*, No. 5, 94–100 (1974).
13. V. Kamath, and A. Prosperetti, "A theoretical study of sonoluminescence," *J. Acoust. Soc. Amer.*, **94**, No. 1, 248–260 (1993).